Korean J. Chem. Eng., 36(9), 1489-1498 (2019)
DOI: 10.1007/s11814-019-0327-6

pISSN: 0256-1115
eISSN: 1975-7220

Development of metal organic framework filled PDMS/PI composite membranes for biobutanol recovery

Aslıhan Çalhan*, Sennur Deniz*, Julio Romero, and Ayça Hasanoğlu*,†**

*Yildiz Technical University, Chem. Eng. Dept., Davutpaşa, Istanbul, Turkey
**University of Santiago de Chile, Chem. Eng. Dept., Santiago, Chile
(*Received 15 February 2019 • accepted 16 June 2019*)

Abstract−Butanol is a second generation biofuel with high potential to replace fossil fuels in the future. The main drawbacks in biobutanol production are the low yields of operation and high cost of separation. In this study, n-butanol recovery from its aqueous solutions was carried out by pervaporation as an alternative separation process using polyimide supported polydimethylsiloxane membranes, which were especially prepared for this purpose. To enhance the separation efficiency of the membrane, metal organic framework fillers of MOF-199 were included in its structure. Several combinations of polyimide supported PDMS active layered membranes were prepared with the fillers in each layer of the membrane, in both layers of membrane and membranes without fillers. Thus, the effect of the fillers on the separation performance was investigated. It was found that the inclusion of MOF-199 enhances the membrane performance; meanwhile, the support layer also contributes to mass transfer of n-butanol. Furthermore, the effect of the process parameters on the pervaporation performance was investigated. Results of pervaporation tests indicate that the developed membranes have a good potential for n-butanol recovery from aqueous mixtures.

Keywords: Butanol Separation, Pervaporation, Polyimide, Polydimethylsiloxane, Metal Organic Framework (MOF)

INTRODUCTION

The separation of butanol from its aqueous mixtures has become an important research interest, especially in the last two decades because of its potential use as a second generation biofuel. Butanol has better fuel properties than ethanol as a renewable biofuel candidate for transportation, and many industries also use it as a feedstock chemical. Thus, separation and purification of butanol is essential for both chemical and biofuel production industries.

The butanol bioproduction is usually known as ABE fermentation since the main solvents produced are acetone, butanol and ethanol. In ABE fermentation the final butanol yield is low due to the severe butanol toxicity to microorganisms. Therefore, it is important to use an efficient separation technique to recover the butanol to overcome the challenge of separating the dilute mixture and compensate for the low yield. Separation techniques of butanol include gas stripping, liquid-liquid extraction, reverse osmosis, adsorption, perstraction and pervaporation [1-3]. Pervaporation is one of the most efficient techniques for separation of dilute organics from aqueous mixtures. For an efficient separation, specific pervaporation membranes with high butanol selectivity must be developed. To enhance the efficiency of the pervaporation separation, mixed matrix membranes (MMMs), which are polymeric membranes with inorganic fillers, have been developed [4-6]. These membranes have the advantages of both organic polymers and inorganic filler phases.

Metal organic frameworks (MOFs) are crystalline nanoporous materials that consist of metal ion clusters or ions and organic linkers. MOFs have gained attention in recent years as they exhibit remarkable properties, such as high surface area, thermal stability, permanent porosity, extraordinary adsorption affinities, large diversity of structure and pore size [4-9]. MOFs have several potential applications, including separation, gas storage, magnets and catalysts [8,9]. MOFs have been widely used as fillers in mixed matrix membranes, especially for gas separation [10-13]. However, their use as fillers in membranes for liquid separation is a relatively new area and only limited number of studies have been reported [4,7,14-22]. According to these studies on the pervaporation separation of organics from aqueous mixtures, pervaporation (PV) performance has been enhanced by incorporation of MOF fillers inside a polymeric matrix. MOF fillers improve the PV performance by several phenomena including changing hydrophobicity/hydrophilicity of the membrane, reducing the resistance of the support layer by giving appropriate controlled voids, giving selective adsorption characteristics to the membrane and improving the affinity with the compound to be separated. The MOF-polymer interaction determines the characteristics of the composite membrane. The use of a hydrophobic MOF filler in a hydrophilic membrane could lead to higher fluxes and lower selectivity due to the voids formed in the polymer matrix. The incorporation of MOFs with similar organic ligands to that of polymer may enhance the selectivity. By choosing the appropriate ligands, the interactions between polymer and filler can be controlled for their use in particular applications. In the literature, several MOF-polymer matrix combinations were studied for organic recovery from aqueous mixtures. Li et al. [7] investigated ZIF-71 filled PDMS membrane for recovery of several types of bioalcohols, including

†To whom correspondence should be addressed.
E-mail: aymeric@yildiz.edu.tr

methanol, ethanol, IPA and sec-butanol, from aqueous mixtures by PV. They reported that the addition of ZIF-71 to PDMS membranes significantly improved both flux and selectivity [7]. Liu et al. [18] added ZIF-71 to the PEBA matrix for recovery of biobutanol in PV. They concluded that the separation factor increased with the filler loading, and the maximum separation factor of 22.3 was achieved at 25 wt% loading [18]. Liu et al. [14] studied Zn(BDC)$(TED)_{0.5}$ (BDC: benzenedicarboxylate, TED: triethylenediamine) incorporating PEBA membranes for biobutanol recovery in PV. They concluded that MMMs enhanced the mechanical properties of the membrane and improved the PV performance [14]. Liu et al. [15] investigated incorporation of ZIF-8 in polymethylphenylsiloxane (PMPS) matrix for isopropanol recovery. They reported that ZIF-8-PMPS membrane exhibited higher selectivity and productivity for recovering isobutanol from water compared with the pure PMPS membrane, indicating that the ZIF-8 nanoparticles create preferential pathways for isobutanol molecules by virtue of their ultrahigh adsorption selectivity [15]. Other studied MOF-polymer membranes for several liquid phase organic separations include $[Cu_2(bdc)_2(bpy)]_n$/SPES-C mixed matrix membranes for separation of methanol/methyl tertbutyl ether mixtures [16], ZIF-7/chitosan membrane for ethanol-water separation [17], ZIF-90/P84 mixed matrix membranes for dehydration of isopropanol [19], Polybenzimidazole (PBI)/ZIF-8 mixed matrix membranes for dehydration of alcohols [20], ZIF-8 membranes deposited onto hollow fiber for desalination [21], ZIF-8, MIL-53(Al), NH2-MIL-53(Al) and MIL-101(Cr) incorporated polyamide (PA)/cross-linked polyimide (PI) membrane for methanol (MeOH) and tetrahydrofuran (THF) separation [22].

Most of the studied MOFs for liquid separation reported in the literature involve zeolitic imidazole frameworks. MOF-199, also known as HKUST-1 or CuBTC, is also a suitable choice of a filler among the MOFs, which contains open metal sites of Cu^{+2} coordinated by carboxylate groups with a highly porous cubic structure. There are several studies on the use of MOF-199 as a filler in membranes for gas separation [23-25]; however, liquid phase separation including pervaporation using membranes with MOF-199 fillers was not much encountered in the literature. Yu et al. [26] applied MOF-199 in PDMS membrane in pervaporative separation of thiophene from model gasoline [26]. They concluded that the channels of CuBTC and the extra free volume cavities at the interface between PDMS matrix and CuBTC particles decrease the permeation resistance, increasing the transmembrane flux. Also, some studies have reported the use of MOF-199 to develop nanocomposite nanofiltration membranes for organic solvent separation [27,28]. These studies indicate that MOF-199 has potential for solvent separation in liquid separations.

In this study, two-layered polymeric composite membranes were developed with polyimide (PI) and polydimethylsiloxane (PDMS), and MOF-199 particles were incorporated in each layer of the membrane to assess the effect of the fillers in the polymer on the separation performance. PI membranes were produced by phase inversion and were coated with PDMS polymer, which is well known for its affinity to organic solvents in pervaporative separations. PI was used as a support layer due to its potential in pervaporation and biofuel separation [29], its compatibility with MOF-199 [27,28,30], high stability and well controlled porous structure. MOF-199 was included in each layer separately and in both layers in order to investigate the effect of the filler in each layer. Pervaporation experiments were carried out to recover butanol from aqueous mixtures with and without filled membranes; and the effect of the several process parameters, such as temperature, hydrodynamic conditions and feed concentration on the membrane performance in terms of transmembrane flux and separation factor, was investigated.

EXPERIMENTAL METHODS

1. Materials

Polyimide (PI) was purchased from Huntsman Advanced Materials and N-methyl-2-pyrrolidone (NMP) used as solvent was supplied by VWR International S.A.S. 1-butanol was purchased from Merck Millipore. Propan-2-ol was purchased from Zag Chemical from Turkey. Polydimethylsiloxane (RTV615A and RTV615B, prepolymer and cross-linking agent respectively) was purchased from GE Bayer Silicons (Leverkusen, Germany). Ethanol was supplied by J.T Baker Avantor Performance Materials. Copper (II) acetate monohydrate (98%, extra pure) and Trimethylamine (99% pure) were purchased from Acros Organics (New Jersey, USA). 1,3,5-Benzenetricarboxylic acid (98%) was obtained from Alfa Aesar (Kandel, Germany). Dimethylformamide (DMF) was purchased from VWR International S.A.S. Dichloromethane (DCM) and n-Hexane were purchased from Lab-Scan Analytical Sciences Ltd.

2. Membrane Preparation

Polyimide (PI) support layers were prepared by phase inversion method. Then PI support layers were coated with polydimethylsiloxane (PDMS) as active layer. The effect of MOF-199 fillers was investigated in each layer of the membrane. First, PI support layer was coated with MOF-199 included PDMS and then with neat PDMS to see the effect of the fillers in the PDMS layer. Accordingly, MOF-199 effect was also investigated in PI layers, and PI layers were made with and without MOF-199. Thus, four types of membranes were prepared and compared: PI/PDMS (without MOF-199), PI/MOF+PDMS (MOF-199 in the active layer), PI+MOF/PDMS (MOF-199 in the support layer), PI+MOF/MOF+PDMS (MOF-199 in both layers).

2-1. MOF-199 Synthesis and MOF-199 Incorporated PDMS Active Layer Preparation

MOF-199 particles (also known as HKUST-1) consist of two main components: 1,3,5 benzenetricarboxylic acid and copper (II) acetate monohydrate. Two solutions were prepared for the synthesis of MOF-199 particles. 1 g of 1,3,5 benzenetricarboxylic acid and 1,612 g of copper (II) acetate monohydrate were dissolved in a mixture of 8 mL of DMF, ethanol and water (8 mL each) by stirring in a vessel. 0.5 mL of trimethylamine was added a few min after these solutions were mixed. Then the solution was stirred for 23 h. Sky-blue colored solution was then washed twice with dimethylformamide (DMF) and three times with dichloromethane (DMC). After, centrifugation was carried out at a speed of 50 rpm for 20 min. The washed MOF-199 particles were placed in a beaker and allowed to dry in a closed area at room temperature. Since the synthesis can be disrupted by moisture in the air, it was kept in a dry ambient.

To prepare the PDMS coating solution, PDMS (RTV 615A) and

50% (wt) of hexane were stirred together using a magnetic stirrer. For MOF-199 incorporated coating solution, the dried particles were weighted at the desired percentage of PDMS polymer (such as 5%, 10%, 20% w/w) and were taken up in hexane. These particles were stirred in hexane using a magnetic stirrer to ensure their homogeneous dispersion. Subsequently, this mixture was added to PDMS at the calculated amounts. The resulting mixture of hexane-particles and PDMS was stirred with a magnetic stirrer for 30 min. After having PDMS (RTV 615A) with or without MOF-199 in hexane, the crosslinking agent of PDMS (RTV 615B) was added to the solution by 10% w/w of the prepolymer. This mixture was mixed in an ultrasonic bath for 30 min before it was coated on the support layer.

2-2. Polyimide Support Layer Preparation by Phase Inversion

Polyimide support layers were prepared with 15% w/w of polyimide solution. N-methyl-2-pyrrolidone (NMP) was used as solvent. 6 g of polyimide was weighted in a container and 33 mL of NMP was added to polyimide. Then, this solution was stirred in a magnetic stirrer for 24 h. The prepared solution was cast onto the glass plate to form the support layer at the desired thickness. The PI layers were prepared with or without MOF-199 particles. For MOF-199 incorporated support layer, the dried MOF-199 particles were added to PI support layer solution by 10% w/w amount of the polyimide. Polyimide support layers were obtained by phase inversion method using a coagulation bath. Two coagulation baths were prepared to complete the polymerization of the PI solution and to remove NMP from the structure. The bath content was determined as 50% v/v of isopropyl alcohol (IPA) in pure water. In this prepared bath, NMP may remain in the PI support layer because it accumulates in the bath. Therefore, a second bath consisting of 50% v/v of IPA in pure water was used. The solution cast on the glass plate was left in the first bath for about 20-30 min, then taken to the second bath and kept for 30 min in this bath. After the membranes were kept sufficiently in the baths, the support layers were thermally treated to remove the solvents in the PI layer, those were water, IPA and NMP. The PI layers were placed between two Teflon plates and put in the oven for heat treatment. First, the heat treatment was carried out at 50 °C for 21 h, and then at 180 °C for 2 h. PI support layer thickness was obtained as 125 μm and the thickness of MOF-199 incorporated PI was obtained as 130 μm within ±8% certainty.

2-3. Membrane Coating

After active layer solutions were prepared as mentioned in Section 2.2.1, the support layers were coated using a spin coating equipment (Laurell Model WS-650MZ-23NPP). The thickness of the active layer consisting of PDMS polymer with and without MOF-199 was 40 μm and 45 μm, respectively. The certainty of the membrane thicknesses was within ±10%.

3. Membrane Characterization

FTIR (Perkin Elmer brand and Spectrum 100 model), DTA/TGA (SII Nanotechnology brand and SII6000 Exstar TG/DTA 6300 model) and BET (Quantachrome brand and Quadrosorb SI model) analyses were performed to characterize the prepared membranes. Morphology analysis was performed by taking the SEM images of the membranes using scanning electron microscopy (Zeiss brand and EVO® LS 10 model). Static water contact angles of the membranes with and without MOF filler were measured (KSV Instruments).

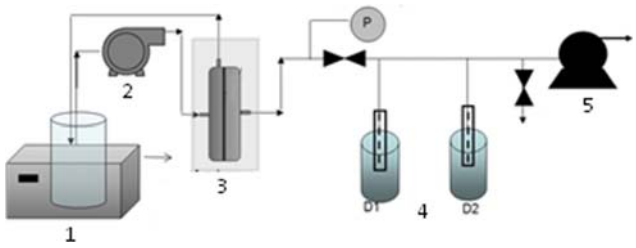

Fig. 1. Experimental setup of pervaporation.

1. Feed tank in water bath
2. Peristaltic pump
3. Membrane cell in isothermal cabin
4. Cold traps of Dewar tanks
5. Vacuum pump

4. Sorption Experiments

Sorption experiments were carried out to determine membrane and filler affinity with butanol and water. The samples of polyimide membrane as well as of PDMS with and without MOF particles with known weight (m_{dry}) were immersed in butanol or water. Everyday samples were taken from the solvent, wiped and weighted until no mass change was observed and this weight was recorded as m_{wet}. Then the sorption degree was calculated from the following equation:

$$\%\text{Sorption} = \frac{m_{wet} - m_{dry}}{m_{dry}} \times 100 \quad (1)$$

5. Pervaporation Experiments

Pervaporation experiments were carried out using the experimental setup shown in Fig. 1. The membrane was placed in a membrane cell kept in a constant temperature cabin. The temperature of the feed solution was set up using a water bath. The feed solution was pumped to the membrane cell and recycled to the feed reservoir. On the downstream side of the membrane, vacuum was applied by a vacuum pump and permeate was collected in a cold trap filled with liquid nitrogen. Every 50 min, the permeate was collected from the cold trap, then weighted, and the transmembrane flux was determined.

Separation factor was estimated from Eq. (2) where y and x represent weight fractions in permeate and in feed, respectively.

$$\alpha = \frac{y_{BuOH}/y_{water}}{x_{BuOH}/x_{water}} \quad (2)$$

RESULTS AND DISCUSSION

1. Intrinsic Properties of the Membranes

1-1. FTIR Analysis

The FTIR analysis of PDMS, PI and MOF-199 was performed and the results are shown in Fig. 2. In the FTIR spectrum of MOF-199, the infrared regions between 1,645-1,590 cm^{-1} and 1,450-1,370 cm^{-1} are attributed the asymmetric and symmetric stretching peaks of carboxylate groups belonging to 1,3,5 benzenetricarboxylic acid. A strong C=O stretching band was observed around 1,640 cm^{-1} in the FTIR spectrum. The peaks around 760 cm^{-1} indicate the pres-

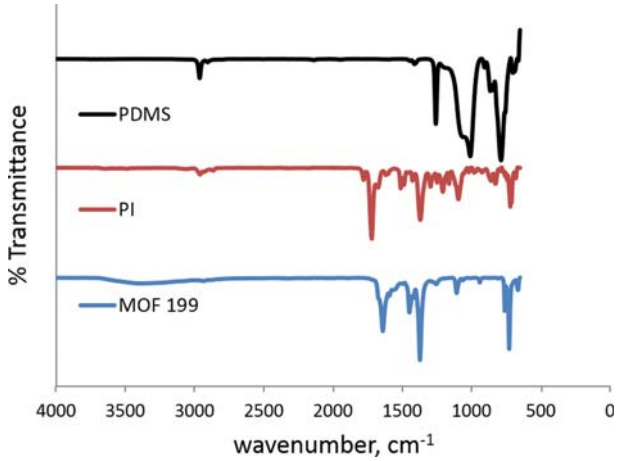

Fig. 2. FTIR spectra of PDMS, polyimide and MOF-199.

ence of copper. The peaks around 1,107 cm^{-1} show C-O-Cu stretching. These results are coherent with the literature [31,32]. In FTIR spectrum of polyimide, absorption bands due to the symmetric and asymmetric C=O stretching vibration of the imide ring and the C-N stretching vibration of the imide bond are located at 1,779, 1,720, and 1,370 cm^{-1}, respectively. These results are in good agreement with the published data on the FTIR spectrum of PI [33,34]. In the FTIR spectrum of PDMS, the characteristic peaks were Si-O-Si stretching at 1,008 cm^{-1}, CH_3 bending in Si-CH_3 at 1,257 cm^{-1}, and CH_3 rocking in Si-CH_3 at 782 cm^{-1}.

1-2. DTA/TGA Analysis

Thermogravimetric analysis (TGA), differential thermal analysis (DTA) and the derivative thermogravimetric analysis (DTG) of the PI, PDMS, MOF-199 and the PI supported MOF-199 included PDMS coated membrane samples were carried out. The samples were heated from room temperature to 850 °C with a heating rate of 10 °C/min under flowing nitrogen. Fig. 3(a) shows the TGA curves of the samples which were obtained by plotting the mass vs. temperature. From the TGA curves, the initial decomposition temperature of the PDMS was determined as around 430 °C, and that of the PI membrane was around 490 °C. In the TGA curve of the MOF-199 sample, two-step decomposition was observed. The first one observed between 80 and 110 °C can be attributed to the

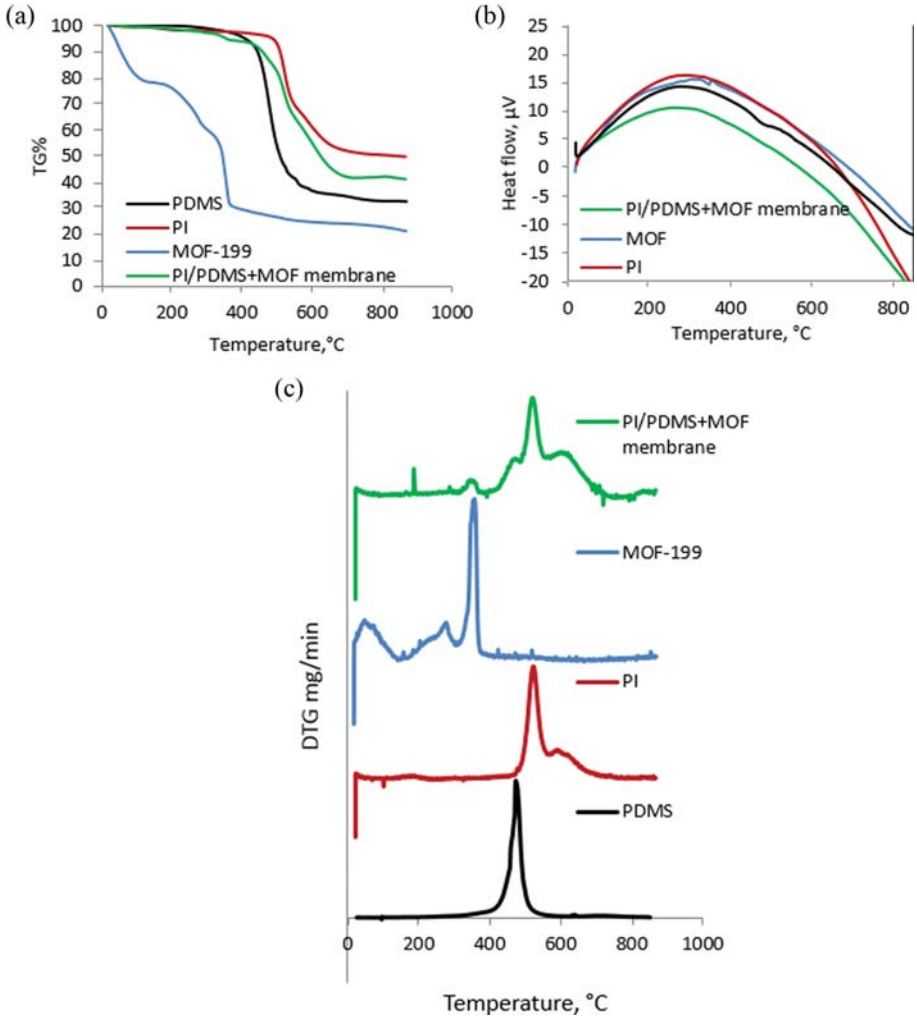

Fig. 3. Thermal analyze results of the PDMS, PI, MOF-199 samples and PI/PDMS+MOF199 membrane (a) TGA curves; (b) DTA curves; and (c) DTG curves.

decomposition of the water and ethanol that remained inside the MOF particles after drying. Also, some fluctuations were observed until 300 °C, which are attributed to the elimination of DMF and the solvents remained in the particles. The main decomposition of the MOF-199 particles was between 310 and 360 °C. The TGA curves of the MOF-199 were compatible with the literature [35]. After the TGA analysis of each polymer and the MOF particles, TGA analysis of the two layered membrane sample with MOF-199 particles was carried out. This TGA curve is coherent with the TGA curves of its components. Fig. 3(b) presents DTA curves of the samples accompanied to the thermal gravity analysis in the temperature range from 25 to 850 °C. The DTA curves of the samples indicate similar patterns with exothermic decomposition behaviors. The DTG traces of the thermograms are given in Fig. 3(c). It can be seen in Fig. 3(c) that the membrane includes all the decomposition peaks of each component.

1-3. BET Analysis

BET analysis was performed at 77 K in nitrogen atmosphere to analyze the pore volume and surface area of the MOF particles by determining nitrogen adsorption. The BET surface area of MOF-199 was determined as 1031.1045 m^2/g. The maximum pore volume was determined as 1.313380 cm^3/g and the micropore volume as 0.918009 cm^3/g. The BET surface area of the synthesized MOF-199 was reported as 950.1274 m^2/g by Brinda et al. [31] and as 1,296 m^2/g by Li and Yang [36]. The BET area determined in this work was in good agreement with the published data.

1-4. XRD Analysis

The crystallinity of the neat PI, PI/MOF-199 and PDMS/MOF-199 composites was examined by XRD in the region of $2\theta=5^o$-55^o, as shown in Fig. 4. From Fig. 4 it can be observed that the PI is an amorphous polymer where the broad hump centered at $2\theta=20^o$ and exhibits no anisotropic behaviors. The amorphous structure of PI was also reported in the literature [33,37]. The XRD pattern of MOF-199 loaded PI composite shows characteristic peaks of PI and some additional peaks belonging to MOF-199 particles. Characteristic peaks of MOF-199 appeared at $2\theta=6.7^o$, 9.5^o, 11.8^o, 13.5^o, 17.5^o, 19.0^o in XRD pattern of composite PI indicating successful production of MOF-199 [31,38]. The PDMS polymer showed basically two diffraction peaks: a first and larger at around 12.0^o and a broader one at around 21.0 °C, reflecting its amorphous property. Similar XRD profiles were previously obtained for PDMS by other

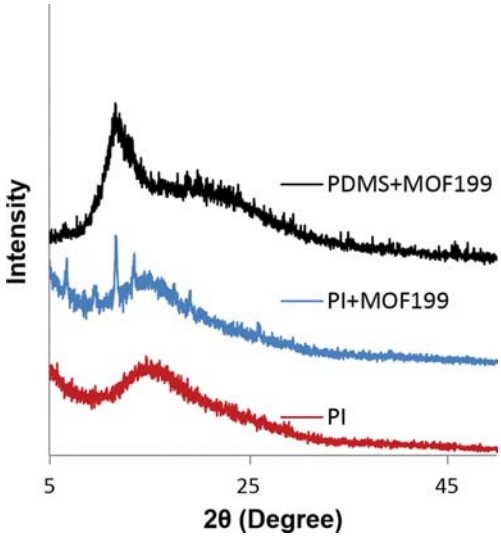

Fig. 4. XRD patterns of neat PI, and MOF-199 incorporated PI and PDMS membranes.

authors, indicating that the fillers did not change the bulk properties of the base material [39]. Some additional peaks belonging to MOF-199 could be also observed in the spectrum of MOF filled PDMS.

1-5. Membrane Structure

The polyimide support membranes were produced at different PI percentages of 10%, 15% and 20% w/w. The SEM images of the PI support layers are given in Fig. 5. In these images the voids formed during phase inversion process of PI layers are finger-like. The porosity and pore size can be controlled by polymer content of the solution. It can be observed from Fig. 5, that the porosity of the polymer decreased with increasing polymer content. Moreover, the PI layers with 15% w/w polymer content were observed to have more homogeneous pore structure. Thus, polyimide concentration was chosen as 15% w/w in NMP for support membrane preparation.

The support layer was coated with PDMS active layer. Fig. 6 shows the SEM images of MOF-199 particles and MOF included PDMS coated PI membrane. It can be seen in Fig. 6 that the PI layer could be coated with PDMS homogeneously and MOF particles were dispersed throughout the PDMS layer.

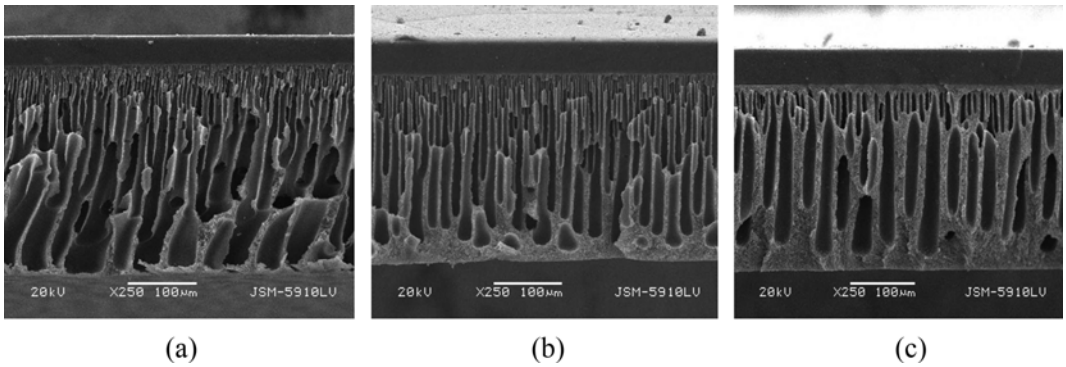

Fig. 5. Cross-sectional SEM images of PI layers (a) 10% w/w, (b) 15% w/w and (c) 20% w/w of PI.

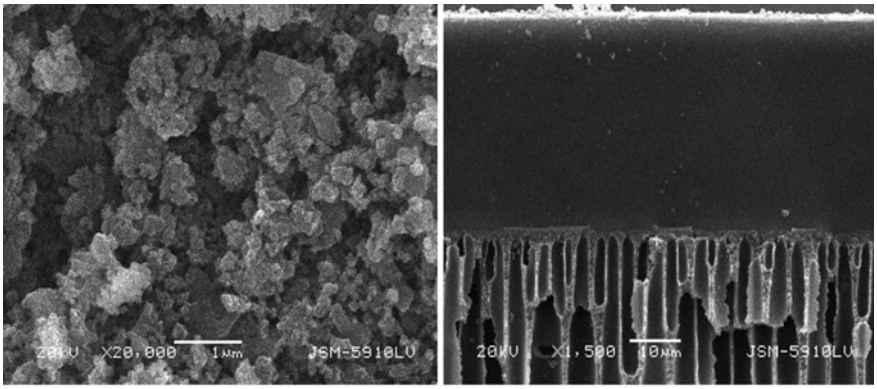

Fig. 6. SEM images of (a) MOF-199 (b) two layered composite PI/PDMS+MOF-199 membrane.

Table 1. Water contact angles of the membranes

Sample	Water contact angle, °
PDMS	109.63
PDMS/MOF-199	114.52
PI	72.77
PI/MOF-199 (10%)	69.39
PI/MOF-199 (20%)	69.81

1-6. Water Contact Angle

The hydrophobicity of the membranes with and without fillers was investigated by water contact angle measurements using 5 μl of drop volume. The contact angles were measured after eight repeats on different points of each sample, and the mean results are reported in Table 1 within 1% certainty. The images of the droplets are given in Fig. 7.

It can be seen from Table 1, that the inclusion of the MOF-199 in PDMS increased the surface hydrophobicity slightly increasing the water contact angle by around 5°. The contact angle of the neat PDMS is found to be coherent with the ones given in the literature, such as 105.5 °C by Ferreira et al. [39] and as 110° by Kanungo et al. [40]. The water contact angle of one MOF-199 pellet has been reported as 60°, which reflects a moderately hydrophilic surface [41]. Therefore, the increase of the contact angle by inclusion of MOF-199 can be attributed to some specific bond interactions between polymer and MOF rather than the hydrophobicity of MOF-199. This contact angle increase can arise from the rotation of hydrophobic methyl groups of PDMS towards the surface because of the attraction between the oxygen bonds of PDMS and Cu sites of MOF-199. Thus, a reorientation of some PDMS groups occurs with MOF inclusion. Also, MOF-199 can give some surface roughness to the PDMS, which may further increase the contact angle [41]. The contact angle increment in hydrophobic membranes with the inclusion of MOF-199 is reported by some researchers. Decoste et al. [42] reported that with the inclusion of MOF-199 in PVDF, the water contact angle was increased from 82° to a range between 84-107° dependent on the filler concentration [42]. Mukherjee et al. [43] reported that PDMS coated MOF-199 pellets exhibited a water contact angle around 130° [43]. However the inclusion of MOF-199 in the PI matrix decreased the water contact angle at an extent of around 3°. This also verifies that the surface wettability of the membrane is affected by the attraction of some specific polymer-filler links rather than the polarity degree of the MOF itself. Also since the two polymers, PDMS and PI, were fabricated by two different methods which are solvent evaporation and phase inversion, the surface roughness given by the MOF-199 is different in each polymer. In phase inversion a dense skin layer is formed on top, where this skin top layer could have a lower roughness when compared to that of a surface formed by the solvent evaporation technique. Moreover the different behavior of MOF fillers inside different polymers shows that MOF-199 has dual polarity characteristics resulting from organic links and active Cu sites.

2. Sorption Results of the Membranes

The butanol and water sorption of PI support layers at different PI concentrations at 30 °C was investigated using the procedure described in Section 2.4, and these results are shown in Fig. 8.

It can be seen from Fig. 8, that the butanol sorption of PI layers was higher than the water sorption, which points out PI layers have more affinity with butanol than with water. As the PI concentra-

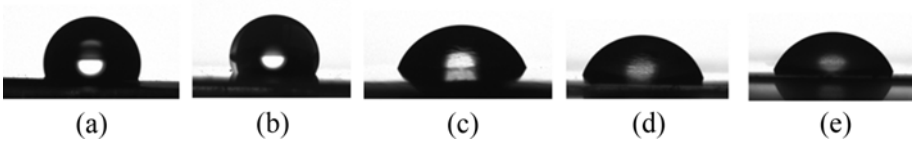

Fig. 7. Images of the water droplets on the membrane surfaces (a) PDMS, (b) PDMS/MOF-199, (c) PI, (d) PI/MOF-199 (10%) and (e) PI/MOF-199 (20%).

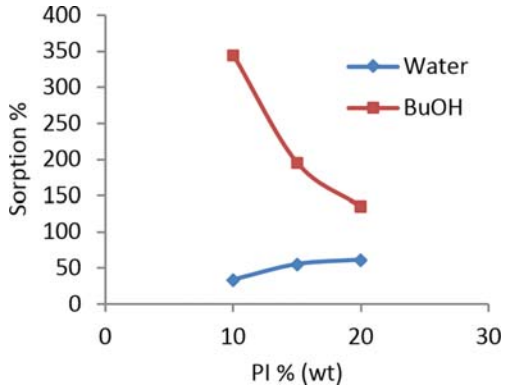

Fig. 8. Effect of the polyimide concentration on water and butanol (BuOH) sorption at 30 °C.

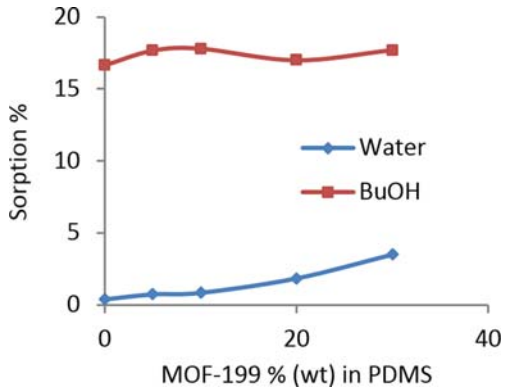

Fig. 9. Effect of MOF-199 concentration in PDMS on water and butanol sorption.

tion increases, butanol sorption decreases and water sorption increases, indicating that PI membrane becomes more hydrophilic with increasing PI concentration. It can be observed from the SEM images of PI layers that the porosity decreases with polymer concentration as it is the case with most polymers. Thus, sorption results indicate that as the porosity decreases, water affinity of the PI membranes increases. Hence, it can be inferred that the porous structure of the PI membrane has an influence on the butanol affinity of the membrane. Although the best butanol sorption and the lowest water sorption was obtained with PI membrane prepared at 10% w/w of PI, the PI concentration for PV membranes was selected as 15% w/w, since the pores were more regular at this concentration and the irregular pore structure at 10% w/w of PI may result in a loss of mechanical strength.

The effect of the MOF-199 concentration in PDMS layers on the water and butanol sorption was investigated. The PDMS membranes were produced at different MOF-199 loadings and membrane sorption in water and butanol was measured. These results are shown in Fig. 9.

According to Fig. 9, sorption percentages of the membranes increased with the increase of MOF-199 loadings in PDMS for both butanol and water as compared to neat PDMS. Nevertheless, this increase in sorption was rather small for butanol, which was around 6%, but relatively higher for water. The water uptake did not change significantly between 0-10% MOF loadings, which was below 0.85%. In this range of MOF loadings the membrane could keep its hydrophobicity as it was also reflected by the water contact angle measurements. But after this MOF content, water sorption increased slightly. Interestingly, MOF-199 shows both polar and apolar characteristics due to its different types of cages in the structure, i.e., cages with Cu sites and without Cu sites. The copper sites result in a more polar behavior of the corresponding cages [44]. The dual behavior of the cages can be also verified with two-step adsorption isotherm of MOF-199 for polar molecules [44,45]. In this study, MOF concentration for PV membranes was chosen as 5% w/w according to the sorption curves obtained for water and butanol.

3. Pervaporation Experiments

Pervaporation experiments were carried out with different membranes. The effect of MOF-199 inclusion in layers, feed concentration, temperature and hydrodynamic conditions on the transmembrane flux and the separation factor was investigated.

3-1. Effect of MOF Inclusion and Feed Concentration

Four different types of PI/PDMS composite membranes were produced with and without MOF-199 (PI/PDMS) where the fill-

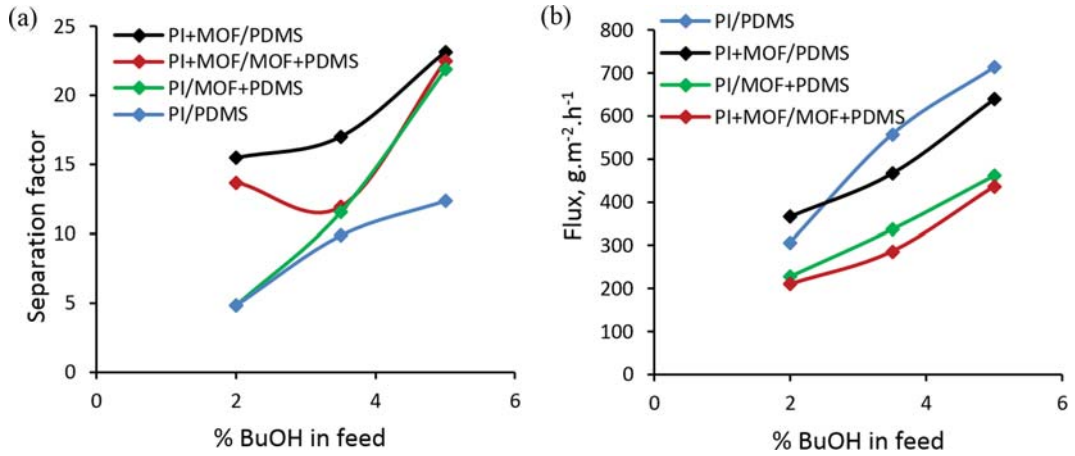

Fig. 10. Pervaporation performance of different membranes as a function of the feed concentration at 30 °C: (a) Separation factor and (b) transmembrane flux.

Table 2. The mean PSI obtained for different membranes at different feed concentrations at 30 °C

	PI/PDMS	PI+MOF/PDMS	PI/MOF+PDMS	PI+MOF/MOF+PDMS
PSI (Jxα)	5277.0	9457.6	5038.9	5372.6

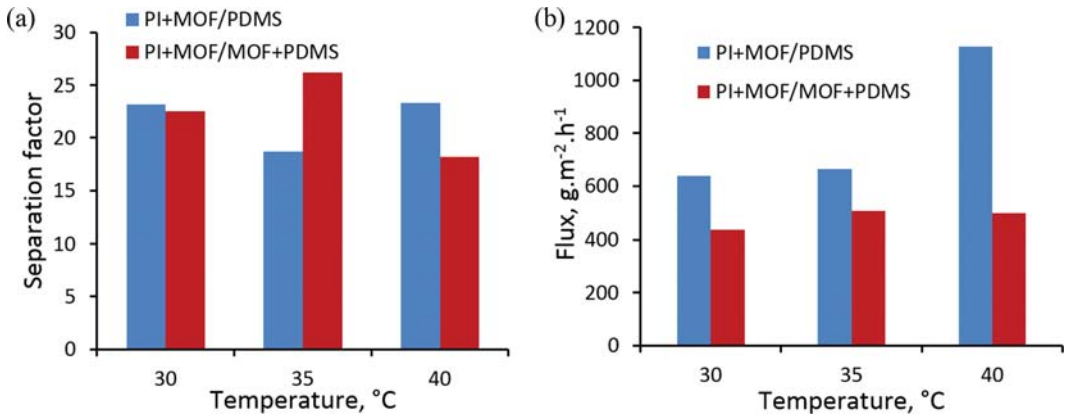

Fig. 11. Pervaporation performance of the composite membranes as a function of temperature at a feed concentration of 5% (w/w): (a) Separation factor and (b) transmembrane flux.

ers were in PDMS layer (PI/MOF+PDMS), in PI layer (PI+MOF/PDMS) and in both layers (PI+MOF/PDMS+MOF). These membranes were used in PV to recover butanol from aqueous solutions at 2.0, 3.5 and 5.0% (w/w) of butanol at 30 °C. The experimental results in terms of transmembrane flux and separation factor are reported in Fig. 10.

According to Fig. 10(a), the inclusion of MOF-199 in any layer gave better separation factor results than the ones obtained using membranes without filler. The presence of the filler in the membrane enhances the preferential permeation of butanol. These results show that the active metal sites and channels of MOF-199 facilitate the transport of butanol. The best results of separation factor were obtained when the fillers were in PI layer. MOF-199 particles in PI layers decrease the permeation resistance with the extra free volume cavities and voids formed in the layer. This may indicate that preferential permeation of butanol through the membrane is mainly controlled by the diffusion rather than sorption mechanism. Pervaporation selectivity is a function of both diffusion and sorption of the components, but can be dominated with one of these mechanisms mainly for specific membrane-component combinations. On the other hand, mean transmembrane fluxes without filler were slightly higher than the ones obtained with the filled membranes. Nevertheless, PI+MOF/PDMS membranes gave relatively higher fluxes. Usually in pervaporation, the separation factor is governed at the cost of flux or vice versa. To optimize the results and make an optimal choice between separation factor and fluxes, pervaporation separation index (PSI) may be used where this can be defined as the product of flux and separation factor, given in Eq. (3) [46]:

$$PSI = J \cdot \alpha \quad (3)$$

For each experiment carried out between 2-5% BuOH at 30 °C, the PSI value was calculated for the given membrane using Eq. (3), and then the mean PSI values were obtained by calculating the arithmetic mean PSI for each membrane. The mean PSI obtained for each membrane is reported in Table 2.

It can be seen in Table 2 that the best PSI value was obtained with PI+MOF/PDMS membrane, which was far better than the other results, followed by PI+MOF/MOF+PDMS membrane. Thus, these two membranes were used for further PV experiments to perform a comparison.

3-2. Effect of Temperature

The pervaporation experiments were carried out using PI+MOF/PDMS and PI+MOF/MOF+PDMS membrane with a feed concentration of 5% (w/w) at different temperatures to investigate the effect of temperature on the transmembrane fluxes. The results are shown in Fig. 11.

Fig. 11(b) shows that the flux tends to increase with the increase of temperature because of the elevated vapor pressure and mobility of the transferred molecules. Also, polymer chains became more flexible at higher temperatures. As a result, the mobility of the polymeric chains increases at higher temperatures and this phenomenon generates extra free volume in the polymer matrix. Consequently, the sorption and diffusion rates of the transported molecules increase. The increase of fluxes with increasing temperatures is more evident in PI+MOF/PDMS membrane than in PI+MOF/MOF+PDMS membrane. Since PDMS is a dense elastomeric membrane, the flexibility of polymer chains and its dependence on temperature is much greater than that of PI membrane. The presence of the MOF-199 in PDMS may hinder the flexibility of the polymer chains and thus the increase in the temperature does not affect the flux as it does in PI+MOF/PDMS membrane. As a result, the change of temperature is more effective in the PI+MOF/PDMS membrane. The mean separation factors of the membranes were very close to each other, which were 21.7 for PI+MOF/PDMS and 22.8 for PI+MOF/MOF+PDMS, although there was a significant difference between the transmembrane flux values. The mean PSI values for each membrane were also calcu-

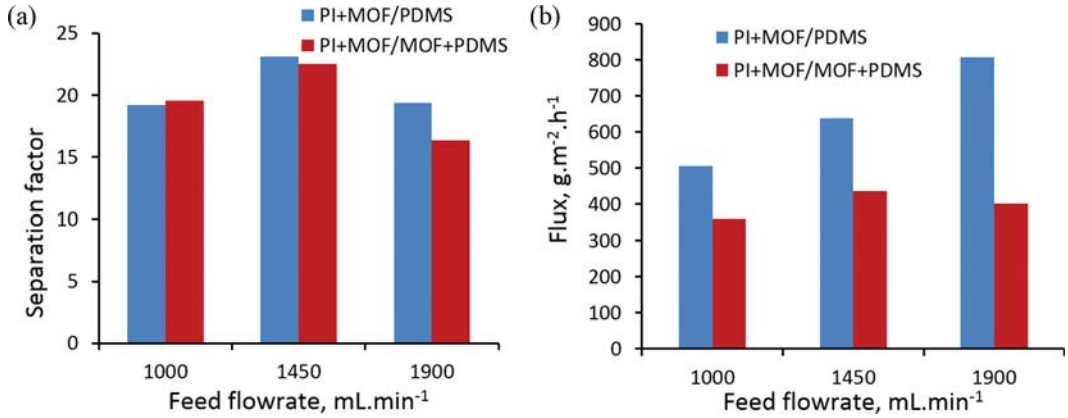

Fig. 12. Pervaporation performance of the composite membranes as a function of feed velocities at 30 °C with a feed concentration of 5% (w/w): (a) Separation factor and (b) transmembrane flux.

lated for the experiments at different temperatures between 30-40 °C with the results given in Fig. 4. The mean PSIs of the membranes at different temperatures were 17587 for PI+MOF/PDMS and 10972 for PI+MOF/MOF+PDMS membrane. The experimental results show that the presence of the MOF particles in PI layers enhances the PV performance.

3-3. Effect of Hydrodynamic Conditions

PV experiments were carried out at different feed velocities in the range of 1,000 to 1,900 mL min^{-1} at 30 °C, with a feed concentration of 5%, in order to investigate the effect of the hydrodynamic conditions on the PV performance. The results are reported in Fig. 12.

In general, an increase of feed flow rate reduces concentration polarization, decreasing the boundary layer thickness, and increases flux due to the reduction of the transport resistance in liquid boundary layer. In pervaporation, since the permeate transport is accelerated by the applied vacuum, there are two main resistances for mass transfer: the feed boundary layer resistance and the membrane resistance. Mass transfer through the membrane may be controlled by mainly one of these resistances or may be influenced by both of them. According to Fig. 12(b), the fluxes of PI+MOF/PDMS membrane increase apparently at higher flow rates. This fact indicates that feed boundary layer resistance has an important contribution to the overall mass transfer resistance for this membrane. On the other hand, when PI+MOF/MOF+PDMS membrane was used at the same feed flow rate conditions, transmembrane fluxes did not change in a significant amount. Thus, it can be inferred that overall mass transfer resistance for this membrane is mainly controlled by resistance represented by the membrane rather than the feed side resistance. From these results obtained with two different membranes, it can be concluded that the presence of the MOF particles in PI layer reduces the membrane resistance; meanwhile, its presence in both layers increases the membrane resistance. The inclusion of MOF particles in the porous structure of PI results in extra voids and free volume. This phenomenon leads to a decrease in the membrane resistance, and as a result PV performance is enhanced. However, when MOF particles are also included in the dense PDMS layer, direct exposure of the MOF particles to aqueous solutions may cause the pores to block. Also the flexibility of the PDMS membrane may be reduced, resulting in a decrease in the PV performance when compared to the PI+MOF/PDMS membrane. The thickness of the membrane is also another important parameter which defines the membrane resistance. Several researchers reported that especially for the elastomeric membranes the selectivity decreases and the flux increases with decreasing membrane thicknesses [47-51]. Thus, a decrease in the active PDMS layer thickness will result in an increase in the fluxes and a decrease in the selectivity. In this study the membrane performance is expected to be more dependent on the active layer thickness rather than the support layer thickness. Since the support layer is porous, the membrane resistance is smaller, besides with the inclusion of the MOF fillers inside the support layer it was experimentally shown that the total membrane resistance was lowered. Thus, a change in the support layer thickness will result in less change in flux compared to the active layer.

The mean separation factor values of the membranes at different feed flow rates were close to each other. The mean PSI values for each membrane at three different flowrates were calculated from the results given in Fig. 12. The mean PSI values of the PI+MOF/PDMS and PI+MOF/MOF+PDMS membranes estimated at different feed velocities were 13389.2 and 7828.6, respectively. The experimental results obtained at all process parameters point out that PI+MOF/PDMS membranes have a good potential for butanol recovery from aqueous mixtures.

CONCLUSION

Pervaporation separation of butanol from aqueous mixtures was carried out using MOF-199 included PI/PDMS composite membranes. The effect of several parameters, such as the influence of the MOF-199 fillers in the membrane layers, temperature, hydrodynamic conditions and feed concentration on the transmembrane flux and separation factor, was investigated. The best PV performance was found when the MOF-199 was included in PI layers. The experimental results showed that the inclusion of MOF-199 in PI layer decreases the membrane resistance and facilitates the preferential transport of butanol. The MOF-199 included PI/PDMS membranes have a good potential for butanol recovery from its aqueous mixtures by pervaporation.

ACKNOWLEDGEMENT

This work was supported by the Research Fund of Yildiz Technical University (Project No: 2015-07-01-KAP03).

NOMENCLATURE

J : flux [$g^{-1}\cdot m^{-2}\cdot h^{-1}$]
x_i : weight fraction of component *i* in feed
PSI : pervaporation separation index
y_i : weight fraction of component *i* in permeate
α : separation factor

REFERENCES

1. N. Abdehagh, F. Handan Tezel and J. Thibault, *Biomass Bioenergy*, **60**, 222 (2014).
2. A. Kujawska, J. Kujawski, M. Bryjak and W. Kujawaski, *Renew. Sust. Energy Rev.*, **48**, 648 (2015).
3. G. Merlet, F. Uribe, C. Aravena, M. Rodriguez, R. Cabezas, E. Quijada-Maldonado and J. Romero, *J. Membr. Sci.*, **537**, 337 (2017).
4. Z. Jia and G. Wu, *Micropor. Mesopor. Mater.*, **235**, 151 (2016).
5. X. Cheng, F. Pan, M. Wang, W. Li, Y. Song, G. Liu, H. Yang, B. Gao, H. Wu and Z. Jiang, *J. Membr. Sci.*, **541**, 329 (2017).
6. Y. K. Ong, G. M. Shi, N. L. Le, Y. P. Tang, J. Zuo, S. P. Nunes and T. S. Chung, *Prog. Polym. Sci.*, **57**, 1 (2016).
7. Y. Li, L. H. Wee, J. A. Martens and I. F. J. Vankelecom, *J. Mater. Chem. A*, **2**, 10034 (2014).
8. R. J. Kuppler, D. J. Timmons, Q. R. Fang, J. R. Li, T. A. Makal, M. D. Young, D. Yuan, D. Zhao, W. Zhuang and H. C. Zhou, *Coord. Chem. Rev.*, **253**, 3042 (2009).
9. K. K. Gangu, S. Maddila, S. B. Mukkamala and S. B. Jonnalagadda, *Inorg. Chim. Acta,* **446**, 61 (2016).
10. B. Zornoza, C. Tellez, J. Coronas, J. Gascon and F. Kapteijn, *Micropor. Mesopor. Mater.,* **66**, 67 (2013).
11. M. R. Abdul Hamid and H. K. Jeong, *Korean J. Chem. Eng.*, **35**, 1577 (2018).
12. S. S. Swain, L. Unnikrishnan, S. Mohanty and S. K. Nayak, *Korean J. Chem. Eng.*, **34**, 2119 (2017).
13. C. Duan, X. Jie, H. Zhu, D. Liu, W. Peng and Y. Cao, *J. Appl. Polym. Sci.*, **135**, 1 (2018).
14. S. Liu, G. Liu, J. Shen and W. Jin, *Sep. Purif. Technol.*, **133**, 40 (2014).
15. X. L. Liu, Y. S. Li, G. Q. Zhu, Y. J. Ban, L. Y. Xu and W. S. Yang, *Angew. Chem. Int. Ed.*, **50**, 10636 (2011).
16. G. L. Han, K. Zhou, T. S. A. N. Lai, Q. G. Zhang, A. M. Zhu and Q. L. Liu, *J. Membr. Sci.*, **454**, 36 (2014).
17. C. H. Kang, Y. F. Lin, Y. S. Huang, K. L. Tung, K. S. Chang, J. T. Chen, W. S. Huang, K. R. Lee and J. Y. Lai, *J. Membr. Sci.*, **438**, 105 (2013).
18. S. N. Liu, G. P. Liu, X. H. Zhao and W. Q. Jin, *J. Membr. Sci.*, **446**, 181 (2013).
19. D. Hua, Y. K. Ong, Y. Wang, T. X. Yang and T. S. Chung, *J. Membr. Sci.*, **453**, 155 (2014).
20. G. M. Shi, T. Yang and T. S. Chung, *J. Membr. Sci.*, **415**, 577 (2012).
21. N. M. Mahpoz, N. Abdullah, M. Z. M. Pauzi, M. A. Rahman, K. H. Abas, A. A. Aziz, M. H. D. Othman, J. Jaafar and A. F. Ismail, *Korean J. Chem. Eng.*, **36**, 439 (2019).
22. S. Sorribas, P. Gorgojo, C. Tellez, J. Coronas and A. G. Livingston, *J. Am. Chem. Soc.*, **135**, 15201 (2013).
23. S. Basu, A. Cano-Odena and I. F. J. Vankelecom, *J. Membr. Sci.*, **362**, 478 (2010).
24. C. J. Duan, X. M. Jie, D. D. Liu, Y. M. Cao and Q. Yuan, *J. Membr. Sci.*, **466**, 92 (2014).
25. H. C. Yoon, P. B. S. Rallapalli, S. S. Han, H. T. Beum, T. S. Jung, D. W. Cho, M. Ko and J. N. Kim, *Korean J. Chem. Eng.*, **32**, 2501 (2015).
26. S. Yu, Z. Jiang, H. Ding, F. Pan, B. Wang, J. Yang and X. Cao, *J. Membr. Sci.*, **481**, 73 (2015).
27. S. Basu, M. Maes, A. Cano-Odena, L. Alaerts, D. E. De Vos and I. F. J. Vankelecom, *J. Membr. Sci.*, **344**, 190 (2009).
28. J. Campbell, G. Székely, R. P. Davies, D. C. Braddock and A. G. Livingston, *J. Mater. Chem.* A, **2**, 9260 (2014).
29. L. Y. Jiang, Y. Wang, T. S. Chung, X. Y. Qiao and J. Y. Lai, *Prog. Polym. Sci.*, **34**, 1135 (2009).
30. S. Sorribas, A. Kudasheva, E. Almendro, B. Zornoza, Ó. Iglesia, C. Téllez and J. Coronas, *Chem. Eng. Sci.*, **124**, 37 (2015).
31. L. Brinda, K. S. Rajan and J. B. B. Rayappan, *J. Appl. Sci.*, **12**, 1778 (2012).
32. R. Khajavian and K. Ghani, *J. Cryst. Growth*, **455**, 60 (2016).
33. B. Chae, D. G. Hong, Y. M. Jung, J. C. Won and S. W. Lee, *Spectrochim. Acta, A Mol. Biomol. Spectrosc.*, **195**, 1 (2018).
34. A. R. Ashraf, Z. Akhter, L. C. Simon, V. McKee and C. D. Castel, *J. Mol. Struct.*, **1160**, 177 (2018).
35. T. T. Li, J. Qianband Yue and Q. Zheng, *RSC Adv.*, **6**, 77358 (2016).
36. Y. Li and R. T. Yang, *AIChE J.*, **54**, 269 (2008).
37. S. Esmaielzadeh and H. Ahmadizadegan, *Solid State Sci.*, **78**, 46 (2018).
38. C. Huang, R. Sun, H. Lu, Q. Yang, J. Hu, H. Wang and H. Liu, *Sep. Purif. Technol.*, **182**, 110 (2017).
39. P. Ferreira, A. Carvalho, T. R. Correia, B. P. Antunes, I. J. Correia and P. Alves, *Sci. Technol. Adv. Mater.*, **14**, 1 (2013).
40. M. Kanungo, S. Mettu and K. Y. Law, *Langmuir*, **30**, 7358 (2014).
41. J. B. Decoste and G. W. Peterson, *Chem. Rev.*, **114**, 5695 (2014).
42. J. B. DeCoste, M. S. Denny, G. W. Peterson, J. J. Mahle and S. M. Cohen, *Chem. Sci.*, **7**, 2711 (2016).
43. S. Mukherjee, S. Sharma and S. K. Ghosh, *APL Mater.*, **7**, 050701 (2019).
44. T. R. C. Van Assche, T. Duerinck, J. J. Guttiérez-Sevillano, S. Calero and J. F. M. Denayer, San Francisco, CA, 13th AIChE Annual Meeting, November (2013).
45. P. Küsgens, M. Rose, I. Senkovska, H. Föde, A. Henschel, S. Siegle and S. Kaskel, *Micropor. Mesopor. Mater.*, **120**, 325 (2009).
46. T. M. Aminabhavi, B. V. K. Naidu, S. Sridhar and R. Rangarajan, *J. Appl. Polym. Sci.*, **95**, 1143 (2005).
47. G. H. Koops, J. A. M. Nolten, M. H. V. Mulders and C. A. Smolders, *J. Appl. Polym. Sci.*, **53**, 1639 (1994).
48. P. Kanti, K. Srigowri, J. Madhuri, B. Smitha and S. Sridhar, *Sep. Purif. Technol.*, **40**, 259 (2004).
49. E. A. Fouad and X. Feng, *J. Membr. Sci.*, **323**, 428 (2008).
50. D. Sun, P. Yang, L. Li, H. H. Yang and B. B. Li, *Korean J. Chem. Eng.*, **31**, 1877 (2014).
51. C. K. Yeom, J. M. Dickson and M. A. Brook, *Korean J. Chem. Eng.*, **13**, 482 (1996).